High-pressure optical study of bromine-doped single-walled carbon nanotube films

J. Strauch[1], B. Anis[1,2], and C. A. Kuntscher[*,1]

[1] Experimentalphysik 2, Universität Augsburg, 86159 Augsburg, Germany
[2] Physics Division, Department of Spectroscopy, National Research Center, Giza 12311, Egypt

[*] Corresponding author: e-mail christine.kuntscher@physik.uni-augsburg.de, Phone: +49 821 5983315, Fax: +49 821 5983411

1 Introduction Single-walled carbon nanotubes (SWCNTs) are well known for their robust mechanical properties due to the strong sp^2 covalent bonds between the carbon atoms. Theoretical prediction as well as previous experimental results indicate a Young's modulus close to 1 TPa for SWCNTs [1, 2]. However, the radial stability of the nanotubes is much lower than the elastic modulus. Due to their soft bulk properties, the nanotubes' cross-section changes from circular to oval or elliptical, and the nanotubes even collapse at high pressure [3].

The mechanical stability of SWCNTs is affected by filling with atoms, molecules, or inner tubes. Earlier high pressure optical studies revealed that a stabilization of SWCNT walls upon filling with inner tubes, C_{60} molecules or iodine occurs [4–6]. In contrast, a high-pressure Raman spectroscopy study considered the iodine filling as a case of inhomogeneous filling, which leads to the destabilization of the nanotubes [7]. The destabilization was ascribed to the non-covalent Van der Waals forces between the nanotube wall and the inner molecules, leading to the instability of the tubes at a low pressure of 1.3 GPa.

Optical spectroscopy is a useful technique for the characterization of the electronic band structure regarding the energy position and spectral weight of the excited optical transitions. Already small pressure-induced deformations of the tubular cross-section can be observed, since the characteristic van Hove singularities (vHs) in the density of states (DOS) of SWCNTs are very sensitive to these deformations [3].

Here, we present a high-pressure optical spectroscopy study on the mechanical stability of bromine-doped SWCNTs (Br-SWCNTs) with different doping levels in comparison with empty SWCNTs. An earlier high-pressure Raman study on Br-SWCNTs showed that most probably bromine as filler molecule occupies preferentially the interstitial channels of the nanotube bundles [8].

2 Experimental Bundled SWCNTs produced by arc discharge were purchased from Carbon Solutions, Inc. (Type P2, average diameter 1.4 nm). Triton X-100 (10% in H_2O) was purchased from Sigma–Aldrich. For the optical spectroscopy study, carbon nanotubes bucky-paper on cellulose nitrate (see Fig. 1a) was prepared using Triton X-100 solution as described in Ref. [9]. The cellulose nitrate was removed by washing with acetone to produce a free-standing SWCNT film. For the preparation of Br-SWCNTs, a small piece of the free-standing SWCNT film is fished with a platinum grid (Hole size 1 mm) (see Fig. 1b). Platinum was used due to the reactivity of bromine. The Pt-grid was inserted into a glass tube with few drops of liquid bromine. The glass tube was

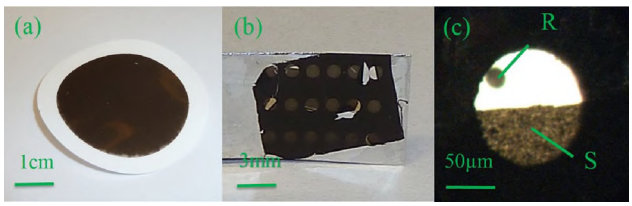

Figure 1 (a) SWCNT film on cellulose nitrate, (b) SWCNT film on Pt-grid, and (c) DAC filled with sample (S) and ruby (R).

sealed and protected from light for 24 h at room temperature. After doping, the glass tube was opened to allow the remaining bromine to evaporate. The Br-SWCNT film was washed with acetone to remove excess bromine from the film. A highly doped sample was prepared by bromine exposure for 24 h (sample A). A second intermediate doped sample was produced by annealing the highly doped sample inside a diamond anvil cell (DAC) (sample B).

Optical spectroscopy measurements were carried out at ambient and high pressure. The transmission measurements on free-standing SWCNT films were performed at room temperature in the energy range 2500–22 000 cm^{-1} with a resolution of 4 cm^{-1}. A Bruker IFS 66v/S Fourier transform spectrometer in combination with an infrared microscope (Bruker IR Scope II) with a 15× Cassegrain objective was used. The pressure was generated using a Syassen–Holzapfel type DAC and determined by the Ruby luminescence technique. Liquid nitrogen was used as hydrostatic pressure transmitting medium. The gasket filled with sample and ruby can be seen in Fig. 1c. The intensity $I_s(\omega)$ of the radiation transmitted through the sample and the reference $I_{ref}(\omega)$ through the pressure transmitting medium in the DAC were measured. The transmittance $T(\omega)$ and absorbance $A(\omega)$ spectra were calculated according to $T(\omega) = I_s(\omega)/I_{ref}(\omega)$ and $A(\omega) = -\log_{10} T(\omega)$, respectively.

The Raman spectra were obtained using a triple Raman spectrometer T64000 (Horiba Jobin Yvon), interfaced to an Olympus BX-40 microscope with a 100× objective. The excitation laser wavelength was 514.5 nm (2.41 eV) from an argon ion laser. The sample was exposed to a laser power of 0.1 mW. The measurements were performed on a powder sample, which was doped for 24 h in liquid bromine.

3 Results and discussion

3.1 Raman spectroscopy Figure 2 depicts the low-frequency region of the Raman spectra for (a) pristine SWCNTs and (b) highly doped Br-SWCNTs. For pristine SWCNTs, the RBMs are located in the range 149.5–184.5 cm^{-1}. The diameter d of the tube is related to the RBM frequency ω_r according to the expression $d = A/\omega_r$. The value of the constant A was assumed to be ≈234, as a mean value of various literature data, hereby neglecting the small effect of the tube–tube interaction [10]. In this case, the uncertainty in the diameter calculation is 5%. Therefore, the diameter distribution of the SWCNTs lies in the range ∼1.27 to 1.57 nm, with an average diameter of ∼1.4 nm.

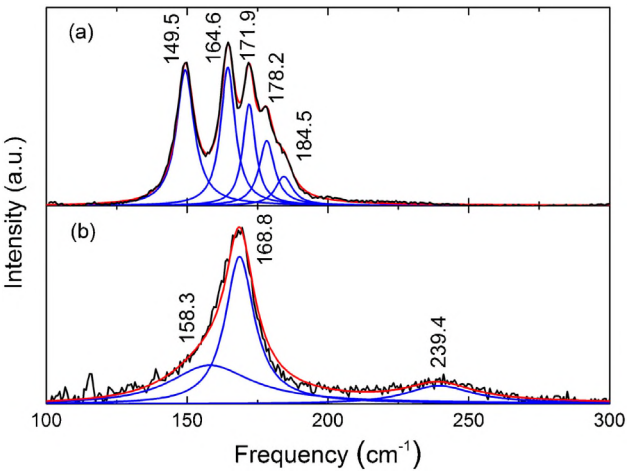

Figure 2 RBM-modes of (a) pristine SWCNT powder and (b) after 24 h doping with bromine. The blue lines are fits of the data with Lorentzian functions. The red line shows the total fit function.

In the case of highly doped Br-SWCNTs (see Fig. 2b), most of the RBM modes are suppressed. This can be attributed to the loss of Raman resonance by hole doping with bromine, whereby electrons are transferred from the π states of the tubes to the bromine molecules. The two peaks at 158.3 and 239.4 cm^{-1} are ascribed to the polybromide chains [8, 11, 12]. The peak at 168.8 cm^{-1} can be attributed to the RBM of the SWCNTs [13, 14].

Figure 3 shows the defect-induced and tangential mode regions of (a) pristine SWCNTs and (b) highly doped Br-SWCNTs. In the frequency region 1300–1450 cm^{-1}, the defect-induced vibration mode (D-mode) is observed. The intensity of the D-band of the Br-doped sample is enhanced; this could be due to adsorbed bromine, which leads to surface functionalization and local deformation of the nanotube

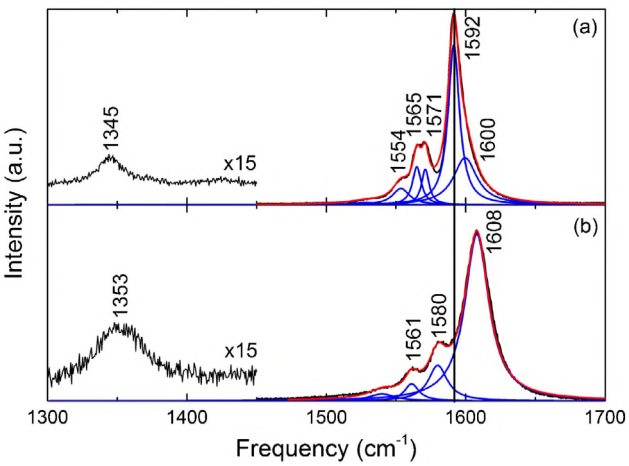

Figure 3 D- and G′-modes of (a) pristine SWCNT powder and (b) after 24 h doping with bromine. The Raman spectra in the range 1300–1450 cm^{-1} in (a) and (b) were multiplied by a factor of 15. The blue lines are fits of the data with Lorentzian functions. The red line shows the total fit function. The Raman spectra were normalized to the intensity of the G-modes.

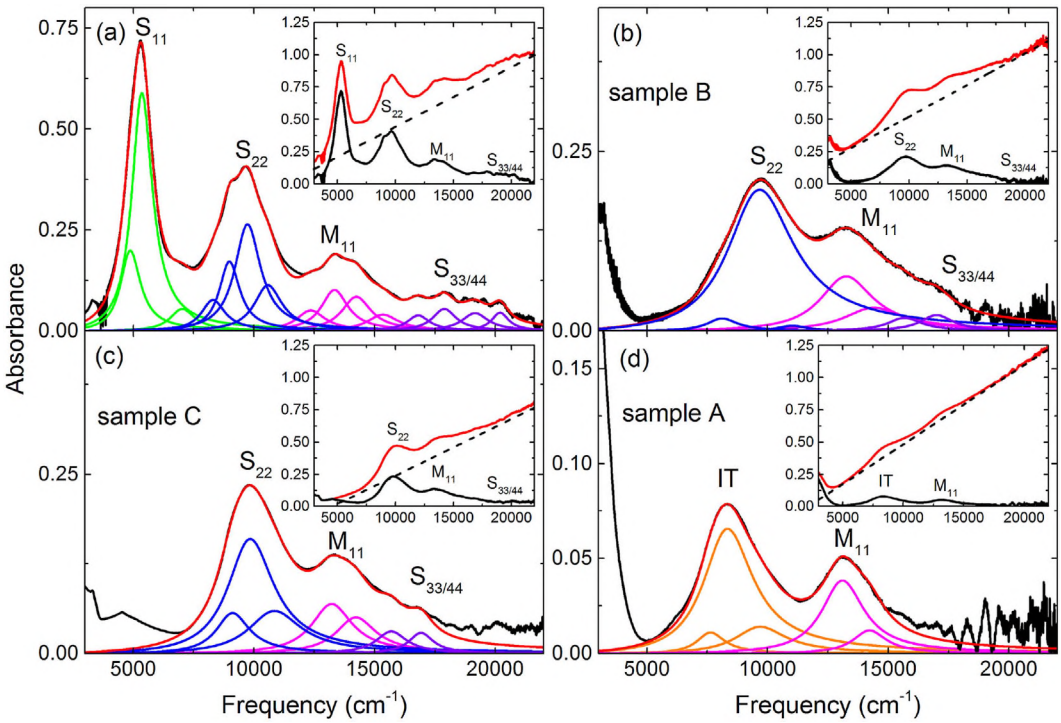

Figure 4 Background-subtracted absorption bands of pristine SWCNTs (a) and Br-SWCNTs (b–d) with different filling ratios: The absorption spectra (black lines) are shown together with the fits (red lines) and the various Lorentz contributions to the fit. The insets illustrate the background-subtraction procedure: The absorbance spectra of SWCNTs before and after background subtraction are plotted together with the linear background (dashed line).

structure. Moreover, a blue shift by $\Delta\nu = 8\,\mathrm{cm}^{-1}$ of the D-band is observed. This shift can be attributed to the doping of the SWCNTs [15].

In the higher-frequency range 1450–1650 cm^{-1}, the G′-modes are observed. In the case of pristine SWCNT the band at 1592 cm^{-1} results mainly from the A_1^{LO}(S) longitudinal mode of the semiconducting tubes (G^+ mode). The bands appearing at 1554, 1565, and 1571 cm^{-1} correspond to the G^- mode. The 1554 cm^{-1} band is ascribed to the E_2^{LO}(M,S) longitudinal mode of the metallic and semiconducting tubes. The bands at 1565 and 1571 cm^{-1} are due to the A_1^{TO}(S,M) transverse mode of the semiconducting and metallic tubes, respectively. The peak at $\sim$1600 cm^{-1} is attributed to the E_2^{TO}(M,S) modes [16–18].

After doping with Br_2 a blue-shift of the G′-band by $\Delta\nu = 7-16\,\mathrm{cm}^{-1}$ can be observed compared to pristine tubes. This shift is generally explained in terms of an electron transfer from the SWCNT to the bromine molecules, generating charged polybromine chains [13, 19–21]. Upon the removal of electrons, the C–C bonds in the nanotubes are stiffened.

3.2 Optical spectroscopy on free-standing Br-SWCNT films Figure 4 shows the background-subtracted absorption bands of pristine SWCNTs and Br-SWCNTs with different filling ratios. The inset of Fig. 4a depicts the complete optical absorbance spectrum of pristine SWCNTs before background subtraction. The spectrum consists of several pronounced absorption bands on top of the broad π–π^* absorption centered at around 5 eV [23]. The background was estimated by a linear function. After background subtraction the absorption bands are clearly visible. The bands labeled S_{ii} and M_{ii} correspond to the i-th optical transitions in semiconducting and metallic nanotubes, respectively (see Fig. 4a). The absorption bands S_{11}, S_{22}, and M_{11} exhibit a fine structure, which results from the nanotube diameter distribution in the sample. The insets in Fig. 4b–d illustrate the background subtraction for the bromine-doped samples.

In the case of the high doping level (see sample A, Fig. 4d), the S_{11} and S_{22} absorption bands disappear, and the intensity of the M_{11} transitions is reduced. A new transition arises at $\sim$8000 cm^{-1}, which corresponds to transitions from deep-lying filled to empty vHs within the valence band [23–25]. These transitions are mapped schematically in Fig. 5a, where the theoretical DOS of semiconducting (10,9) and metallic (10,10) tubes with diameters of approximately 1.4 nm is plotted. The vHs are labeled with v and c for valence and conduction bands, respectively, and the subscripts s and m refer to semiconducting and metallic tubes, respectively. In the case of high doping, electrons are removed completely from v_s^1, v_s^2, and partially from v_m^1. Therefore, the Fermi energy E_F is shifted below v_m^1. Due to the presence of empty valence states intraband transitions occur. The arrows labeled with IT depict the possible intraband transitions [23–25].

For intermediate doping (sample B, see Fig. 4b), the S_{11} absorption band is completely suppressed and the intensity

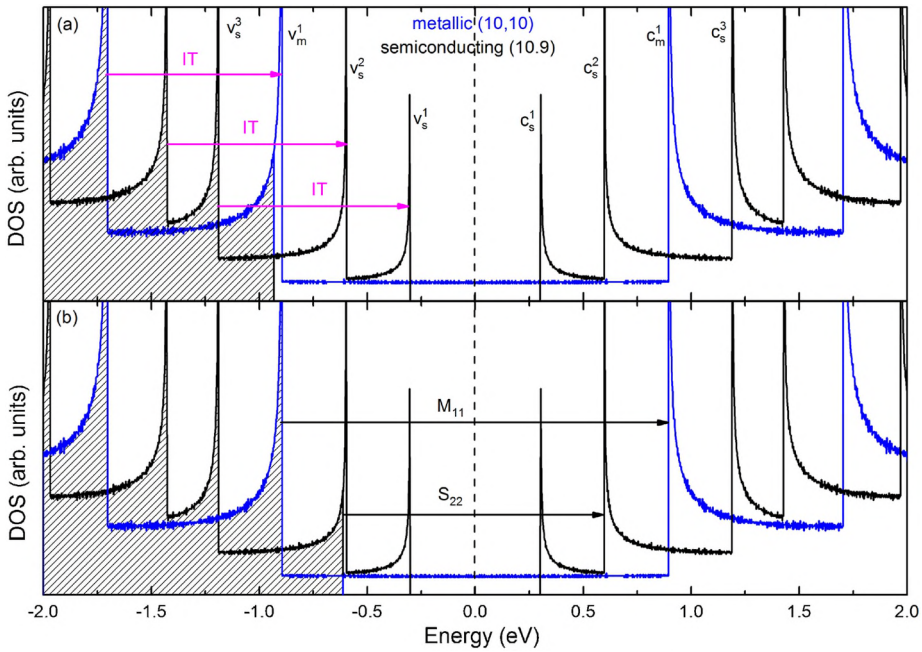

Figure 5 Theoretically calculated DOS of metallic (10,10) (blue) and semiconducting (10,9) (black) SWCNTs. (a) Intraband transitions (ITs) in sample A and (b) optical transitions in sample B [22].

of the S_{22} band is reduced compared to pristine SWCNTs, consistent with earlier reports of SWCNTs filled with various electron acceptors [13, 26, 27]. This can be explained by the removal of electrons from the valence band. First, the v_s^1 vHs is completely depleted and then the v_s^2 vHs is partially depleted; thus, E_F is shifted below v_s^2 (see Fig. 5b). Therefore, the S_{11} transitions disappear and the intensity of the S_{22} band is reduced. The allowed transitions S_{22} and M_{11} can be seen in Fig. 5b marked by arrows.

To prove that the heat treatment removes bromine from the sample, another sample has been prepared with a doping duration of 6 h (sample C, see Fig. 4c). This absorption spectrum is consistent with that of the sample with intermediate doping. There is only a small red shift and damping of the features in the spectrum of sample B compared to the 6 h doped sample C. This could be due to the small initial pressure in the DAC (see annealing procedure described in Section 2).

3.3 Optical spectroscopy of Br-SWCNTs under pressure Figure 6 shows the background-subtracted optical absorption spectra for pristine SWCNTs and the Br-doped samples A and B for selected pressures. For the doped sample the maximum applied pressure was 15 GPa. The contributions to the absorption spectra are illustrated in the insets of Fig. 6a–c, where the absorption spectrum for each sample is plotted together with the Lorentz contributions and the total fitting curve. In the following analysis, only the strong Lorentz contributions were considered. The spectrum of the pristine SWCNT sample has many strong contributions: one for the S_{11}, two for the S_{22}, and two for the M_{11} optical transitions. In the case of the doped sample B, only

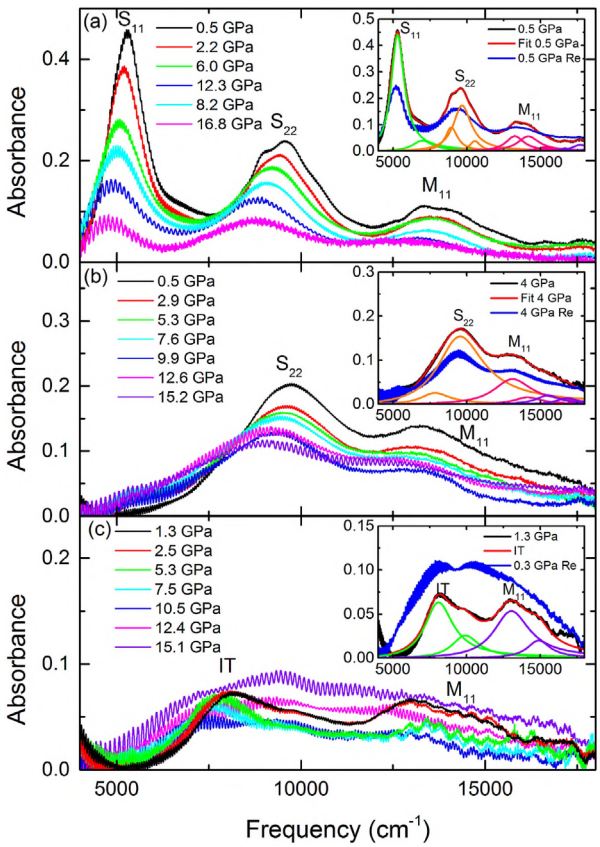

Figure 6 Absorption bands of the SWCNT films in the DAC with increasing pressure: (a) pristine SWCNTs, (b) Br-doped SWCNTs with low doping level (sample B), and (c) heavily Br-doped SWCNTs (sample A).

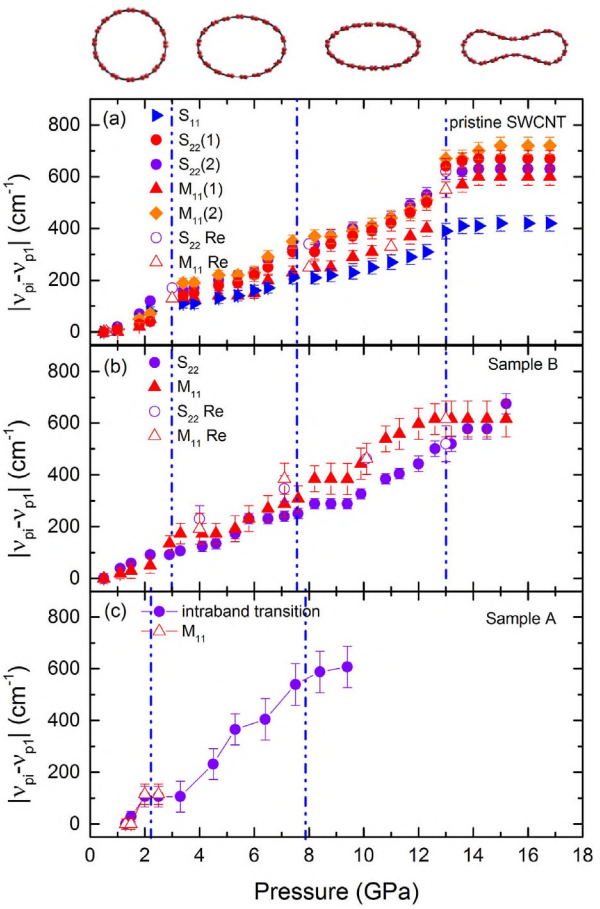

Figure 7 Pressure-dependent relative energy shifts of the optical transitions in (a) pristine SWCNTs, (b) Br-doped SWCNTs with low doping level (sample B), and (c) heavily Br-doped SWCNTs (sample A)

one contribution was considered for the S_{22} and one for the M_{11} absorption band. Also for sample A, one Lorentz contribution for the intraband transitions and one for the M_{11} band were considered in the following.

According to Fig. 6, one finds a red-shift under pressure for the absorption bands in pristine and Br-doped SWCNTs. This was also reported in earlier studies [3], and arises from σ^*–π^* hybridization and symmetry breaking [28–30]. Furthermore the absorption bands exhibit a significant broadening and a pronounced reduction in intensity. For pristine SWCNTs and sample B all optical transitions are resolvable up to the highest applied pressure (16.8 and 15.2 GPa, respectively). For sample A, the ITs and the M_{11} can no longer be resolved above 10 and 2.5 GPa, respectively.

For a quantitative analysis, the relative energy shifts of the Lorentzian contributions are plotted as a function of applied pressure in Fig. 7. The pressure-induced shift of the pristine SWCNT film (see Fig. 7a) exhibits a change in slope at the critical pressures $P_{c1} \approx 3$ GPa, $P_{c2} \approx 7.5$ GPa, and $P_{c3} \approx 13$ GPa. According to earlier high-pressure optical spectroscopy results and theoretical studies [3, 5, 31–35], we interpret the anomaly at P_{c1} as the result of a structural phase transition from a circular to an oval cross-section. The anomaly at P_{c2} signals a deformation from oval to race-track or peanut shape structure. The rapid increase in the relative shift above 11 GPa was interpreted as the onset of the structural collapse, which is completed at 13 GPa [5]. The proposed structural deformation of SWCNTs is shown on top of Fig. 7. For sample A (high Br_2-doping) and sample B (intermediate Br_2-doping) the pressure-induced anomalies can be found in the same pressure range as for the pristine sample (see Fig. 7b and c). Obviously, the bromine doping does not affect the structural stability of the nanotubes. This could be a consequence of the favorable arrangement of bromine as polymer chains in the nanotube interstitial channels: The location of the adsorbed bromine was investigated in a previous high-pressure Raman spectroscopy study on Br-SWCNTs, and it was reported that most probably Br_3^- and Br_5^- bromine polymer chains are formed, which are located in the interstitial channels between the nanotubes [8]. Furthermore, it was shown that bromine can be used for the separation and purification of carbon nanoparticles due to the intercalation of bromine in interstitial channels [36]. This leads to a separation of the carbon structures after annealing the sample.

The insets of Fig. 6 also depict the absorbance spectra at the lowest pressure during pressure release. For pristine SWCNTs and the intermediately doped sample B, the pressure-induced frequency shifts of the optical transitions are reversible upon pressure release. However, a loss in intensity of up to 50% of the original value is observed. The irreversible changes indicate a permanent deformation of the nanotubes during pressure loading. For the highly-doped sample, it is difficult to estimate the frequency position and the loss in the intensity of the absorption bands upon pressure release because of the strong broadening of the features in the spectrum.

4 Summary Br-doped SWCNT samples have been prepared and characterized by optical and Raman spectroscopy. The charge doping of the nanotubes by bromine is revealed by shifts of the Raman modes, the intensity reduction of the absorption bands, and the appearance of intraband transitions. The structural stability of bromine-doped SWCNTs under hydrostatic pressure has been characterized in terms of the optical transitions. The relative frequency shifts show anomalies in the same pressure regimes as for pristine SWCNTs. Thus, the mechanical stability seems to be unaffected by bromine doping. This can be explained by the intercalation of bromine polymer chains in the interstitial channels of the SWCNT bundles.

Acknowledgements We thank M. Schreck and M. Weinl, Experimentalphysik 4, Universität Augsburg, for the Raman measurements. We acknowledge financial support by the DFG (KU 1432/3-2).

References

[1] J. Lu, Phys. Rev. Lett. **79**, 1297 (1997).
[2] B. Peng, M. Locascio, P. Zapol, S. Li, S. L. Mielke, G. C. Schatz, and H. D. Espinosa, Nature Nanotechnol. **3**, 626 (2008).
[3] K. Thirunavukkuarasu, F. Hennrich, K. Kamarás, and C. A. Kuntscher, Phys. Rev. B **81**, 045424 (2010), and references therein.
[4] B. Anis, K. Haubner, F. Börrnert, L. Dunsch, M. H. Rümmeli, and C. A. Kuntscher, Phys. Rev. B **86**, 155454 (2012).
[5] B. Anis, F. Börrnert, M. H. Rümmeli, and C. A. Kuntscher, J. Phys. Chem. C **117**, 21995 (2013).
[6] B. Anis, PhD Thesis, Institut für Physik, Universität Augsburg (2013).
[7] A. L. Aguiar, E. B. Barros, R. B. Capaz, A. G. Souza Filho, P. T. C. Freire, J. M. Filho, D. Machon, C. Caillier, Y. A. Kim, H. Muramatsu, M. Endo, and A. San-Miguel, J. Phys. Chem. C **115**, 5378 (2011).
[8] B. Liu, Q. Cui, M. Yu, G. Zou, J. Carlsten, T. Wågberg, and B. Sundqvist, J. Phys.: Condens. Matter **14**, 11255 (2002).
[9] Z. Wu, Science **305**, 1273 (2004).
[10] S. Bandow, G. Chen, G. Sumanasekera, R. Gupta, M. Yudasaka, S. Iijima, and P. Eklund, Phys. Rev. B **66**, 075416 (2002).
[11] A. Schnittke, H. Stegemann, H. Füllbier, and J. Gabrusenoks, J. Raman Spectrosc. **22**, 627 (1991).
[12] S. Matsuzaki, T. Kyoda, T. Ando, and M. Sano, Solid State Commun. **67**, 505 (1988).
[13] A. Eliseev, L. Yashina, M. Brzhezinskaya, M. V. Chernysheva, M. V. Kharlamova, A. V. Verbitsky, N. I. Lukashin, N. A. Kiselev, A. S. Kumskov, R. M. Zakalyuhin, J. L. Hutchison, B. Freitag, and A. S. Vinogradov, Carbon **48**, 2708 (2010).
[14] M. V. Kharlamova, L. V. Yashina, A. A. Volykhov, J. J. Niu, V. S. Neudachina, M. M. Brzhezinskaya, T. S. Zyubina, A. I. Belogorokhov, and A. A. Eliseev, Phys. Status Solidi B **34**, 85 (2012).
[15] L. G. Bulusheva, A. V. Okotrub, E. Flahaut, I. P. Asanov, P. N. Gevko, V. O. Koroteev, Y. V. Fedoseeva, A. Yaya, and C. P. Ewels, Chem. Mater. **24**, 2708 (2012).
[16] V. Popov and P. Lambin, Phys. Rev. B **73**, 165425 (2006).
[17] H. Rauf, T. Pichler, R. Pfeiffer, F. Simon, H. Kuzmany, and V. Popov, Phys. Rev. B **74**, 235419 (2006).
[18] A. Jorio, G. Dresselhaus, M. Dresselhaus, M. Souza, M. Dantas, M. Pimenta, A. Rao, R. Saito, C. Liu, and H. Cheng, Phys. Rev. Lett. **85**, 2617 (2000).
[19] M. V. Kharlamova, Phys. Uspekhi **56**, 1047 (2013).
[20] A. Rao, P. Eklund, S. Bandow, A. Thess, and R. Smalley, Nature **388**, 257 (1997).
[21] L. Grigorian, K. Williams, S. Fang, G. Sumanasekera, A. Loper, E. Dickey, S. Pennycook, and P. Eklund, Phys. Rev. Lett. **81**, 5560 (1998).
[22] http://www.photon.t.u-tokyo.ac.jp/∼maruyama/kataura/1D_DOS.html [accessed January 20, 2014].
[23] N. Minami, S. Kazaoui, R. Jacquemin, H. Yamawaki, K. Aoki, H. Kataura, and Y. Achiba, Synth. Met. **116**, 405 (2001).
[24] R. Jacquemin, S. Kazaoui, D. Yu, A. Hassanien, N. Minami, H. Kataura, and Y. Achiba, Synth. Met. **115**, 283 (2000).
[25] S. Kazaoui, N. Minami, R. Jacquemin, H. Kataura, and Y. Achiba, Phys. Rev. B **60**, 13339 (1999).
[26] M. V. Kharlamova, Appl. Phys. A **111**, 725 (2013).
[27] T. Takenobu, T. Takano, M. Shiraishi, Y. Mukakami, M. Ata, H. Kataura Y. Achiba, and Y. Iwasa, Nature Mater. **69**, 683 (2003).
[28] J. Wu, W. Walukiewicz, W. Shan, E. Bourret-Courchesne, J. Ager, K. Yu, E. Haller, K. Kissell, S. Bachilo, R. Weisman, and R. Smalley, Phys. Rev. Lett. **93**, 017404 (2004).
[29] J. Charlier, P. Lambin, and T. Ebbesen, Phys. Rev. B **54**, R8377 (1996).
[30] G. Liu, X. Wang, J. Chen, and H. Lu, Phys. Status Solidi B **245**, 689 (2008).
[31] S. P. Chan, W. L. Yim, X. Gong, and Z. F. Liu, Phys. Rev. B **68**, 075404 (2003).
[32] M. Sluiter and Y. Kawazoe, Phys. Rev. B **69**, 224111 (2004).
[33] M. Hasegawa and K. Nishidate, Phys. Rev. B **74**, 115401 (2006).
[34] M. Peters, L. McNeil, J. Lu, and D. Kahn, Phys. Rev. B **61**, 5939 (2000).
[35] C. A. Kuntscher, A. Abouelsayed, K. Thirunavukkuarasu, F. Hennrich, and Y. Iwasa, Phys. Status Solidi B **247**, 2789 (2010).
[36] Y. K. Chen, M. L. H. Green, J. L. Griffin, J. Hammer, R. M. Lago, and S. C. Tsang, Adv. Mater. **8**, 1012 (1996).